Super-Liquid-Repellent Surfaces Prepared by Colloidal Silica Nanoparticles Covered with Fluoroalkyl Groups

Masaya Hikita,[†,‡] Keiji Tanaka,[§] Tetsuya Nakamura,[‡] Tisato Kajiyama,*[,∥] and Atsushi Takahara*[,⊥]

Japan Chemical Innovation Institute (JCII), 1-3-5 Kanda-Jimbocho, Chiyoda-ku, Tokyo 101-0051, Japan, and Department of Applied Chemistry and Institute for Materials Chemistry and Engineering, Kyushu University, Fukuoka 812-8581, and NOF Corporation, Aichi 470-2398, Japan

Received April 5, 2005. In Final Form: April 24, 2005

A simple and easy method to prepare super-liquid-repellent surfaces is proposed. Sol−gel films were prepared by hydrolysis and condensation of alkoxysilane compounds. Both surface energy and roughness were controlled using colloidal silica particles and fluoroalkylsilane. When the fractional amounts of both colloidal silica and fluoroalkylsilane were optimized in the films, the film surface exhibited repellency to both water and oil. Finally, it was shown that the method proposed here would be applied to a simple one-pot coating for a uniform large area, and be useful for practical use.

Introduction

Surface energy is one of the most important properties of polymers and influences a material's wettability, adhesion properties, friction properties, etc.[1−3] In general, to what extent a material is wet with a liquid is governed by the balance of surface free energy and roughness.[4,5] A fundamental framework of this issue has been independently established by Wenzel and Cassie.[6,7] The difference between the two approaches is how a probe liquid contacts the surface. In Wenzel's approach, the liquid fully penetrates the surface grooves, so-called homogeneous wetting. On the other hand, Cassie proposed a notion of heterogeneous wetting; the liquid does not get into the grooves because of trapped air. That is, the hills and valleys at the surface are in contact with the liquid and the air, respectively. Either way, increasing surface roughness makes the contact angle larger, although the contact angle must be higher than 90° for Wenzel's approach.

In the 1950s, primitive and simple trials to increase the water contact angle have been carried out.[8] Since then, superhydrophobic surfaces have been successfully prepared by controlling both surface chemistry and roughness. To accomplish this goal, surface energy should be decreased to as low a value as possible. This can be accomplished by partitioning lower surface energy species to the surface. A typical example of such an approach is to use fluoroalkylsilane or multicomponent polymers containing fluorine. In contrast, we now know that it is not trivial to design and fabricate the surfaces with appropriate roughness characteristics.[9−12] To date, various procedures to provide surface roughness have been carried out. For instance, experiments on the basis of filler addition,[13] plasma etching and polymerization,[14−18] chemical vapor deposition,[19−21a] fluoride particle plating,[21b,22] molding,[23] solidification,[24,25] solution−precipitation reaction in hot water,[26] and phase separation[27−29] have been reported. However, these conventional methods need multisteps and sometimes are quite complicated, meaning

* To whom correspondence should be addressed: Fax: +81-92-651-5606 (T.K.), +81-92-642-2715 (A.T.). Phone: +81-92-642-2100 (T.K.), +81-92-642-2721 (A.T.). E-mail: kajiyama@cstf.kyushu-u.ac.jp (T.K.), takahara@cstf.kyushu-u.ac.jp (A.T.).

† JCII.

‡ NOF Corp.

§ Department of Applied Chemistry, Kyushu University.

∥ Kyushu University.

⊥ Institute for Materials Chemistry and Engineering, Kyushu University.

(1) Schrader, M.; Loeb, G. *Modern approach to wettability: theory and applications*; Plenum Press: New York, 1992.

(2) Garbassi, F.; Morra, M.; Occhiello, E. *Polymer surfaces from physics to technology*; Wiley: Chichester, U.K., 1994.

(3) Jones, R. A. L.; Richards, R. W. *Polymers at surfaces and interfaces*; Cambridge University Press: Cambridge, U.K., 1999.

(4) Johnson, R. E.; Dettre, R. H. *Adv. Chem. Ser.* **1963**, *43*, 112.

(5) Adamson, A. W.; Gast, A. P. *Physical chemistry of surfaces*, 6th ed.; Wiley: New York, 1997.

(6) Wenzel, R. N. *Ind. Eng. Chem.* **1936**, *28*, 988.

(7) Cassie, A. B. D.; Baxter, S. *Trans. Faraday Soc.* **1944**, *40*, 546.

(8) Bartell, F. E.; Shepard, J. W. *J. Phys. Chem.* **1953**, *57*, 211.

(9) Öner, D.; McCarthy, T. J. *Langmuir* **2000**, *16*, 7777.

(10) Yoshimitsu, Z.; Nakajima, A.; Watanabe, T.; Hashimoto, K. *Langmuir* **2002**, *18*, 5818.

(11) (a) Patankar, N. A. *Langmuir* **2003**, *19*, 1249. (b) He, B.; Patankar, N. A.; Lee, J. *Langmuir* **2003**, *19*, 4999.

(12) Marmur, A. *Langmuir* **2004**, *20*, 3517.

(13) Sasaki, H.; Shouji, M. *Chem. Lett.* **1998**, 293.

(14) Washo, B. D. *Org. Coat. Appl. Polym. Sci. Proc.* **1982**, *47*, 69.

(15) Morra, M.; Occhiello, E.; Garbassi, F. *Langmuir* **1989**, *5*, 872.

(16) Youngblood, J. P.; McCarthy, T. J. *Macromolecules* **1999**, *32*, 6800.

(17) Jung, D.-H.; Park, I. J.; Choi, Y. K.; Lee, S.-B.; Park, H. S.; Rühe, J. *Langmuir* **2002**, *18*, 6133.

(18) Woodward, I.; Schofield, W. C. E.; Roucoules, V.; Badyal, J. P. S. *Langmuir* **2003**, *19*, 3432.

(19) (a) Hozumi, A.; Takai, O. *Thin Solid Films* **1997**, *303*, 222. (b) Hozumi, A.; Takai, O. *Thin Solid Films* **1998**, *334*, 54.

(20) Genzer, J.; Efimenko, K. *Science* **2000**, *290*, 2130.

(21) (a) Miller, J. D.; Veeramasuneni, S.; Drelich, J.; Yalamanchili, M. R.; Yamauchi, G. *Polym. Eng. Sci.* **1996**, *36*, 1849. (b) Veeramasuneni, S.; Drelich, J.; Miller, J. D.; Yamauchi, G. *Prog. Org. Coat.* **1997**, *265*, 31.

(22) Kunugi, Y.; Nonaku, T.; Chong, Y.-B.; Watanabe, N. *J. Electroanal. Chem.* **1993**, *353*, 209.

(23) Bico, J.; Marzolin, C.; Quere, D. *Europhys. Lett.* **1999**, *47*, 220.

(24) (a) Onda, T.; Shibuichi, S.; Satoh, N.; Tsujii, K. *Langmuir* **1996**, *12*, 2125. (b) Shibuichi, S.; Onda, T.; Satoh, N.; Tsujii, K. *J. Phys. Chem.* **1996**, *100*, 19512. (c) Tsujii, T.; Yamamoto, T.; Onda, T.; Shibuichi, S. *Angew. Chem., Int. Ed. Engl.* **1997**, *36*, 1011.

(25) Feng, L.; Li, S.; Li, H.; Zhai, J.; Song, Y.; Jiang, L.; Zhu, D. *Angew. Chem., Int. Ed.* **2002**, *41*, 1221.

(26) (a) Tadanaga, K.; Katata, N.; Minami, T. *J. Am. Ceram. Soc.* **1997**, *80*, 3213. (b) Tadanaga, K.; Kitamuro, K.; Morinaga, J.; Kotani, Y.; Matsuda, A.; Minami, T. *Chem. Lett.* **2000**, 864.

(27) Nakajima, A.; Abe, K.; Hashimoto, K.; Watanabe, T. *Thin Solid Films* **2000**, *376*, 140.

(28) Erbil, H. Y.; Demirel, A. L.; Avci, Y.; Mert, O. *Science* **2003**, *299*, 1377.

(29) Xie, Q.; Xu, J.; Feng, L.; Jiang, L.; Tang, W.; Luo, X.; Han, C. C. *Adv. Mater.* **2004**, *16*, 302.

10.1021/la050901r CCC: $30.25
Published on Web 07/09/2005

that they cannot be easily scaled up to practical systems. In contrast to the works mentioned above, Miller and coworkers proposed one-step methods to prepare superhydrophobic coatings.[21] In their experiment, poly(tetrafluoroethylene) rough surfaces were prepared on glass plates by a technique of vacuum deposition or a plating method.[21] Although they could successfully prepare a super-water-repellent surface, unfortunately, it was not possible to coat uniformly large samples.

In this paper, we propose a simple one-step coating process to prepare superhydrophobic surfaces with a large area. The surface obtained by our method exhibited super-repellency to oil as well. To the best of our knowledge, this is the first report dealing with how to prepare the surface with super-repellency to oil as well as water. In addition, the transparency and durability of the super-liquid-repellent layer made it good enough to be practically used. This result is also superior to outcomes from other experiments with superhydrophobic surfaces briefly reviewed above.

Experimental Section

Materials. Tetraethyl orthosilicate (TEOS), colloidal silica (IPA-ST, solid contents 30 wt %, 2-propanol dispersion solution), and (heptadecafluoro-1,1,2,2-tetrahydrodecyl)triethoxysilane (FOETES) were purchased from Tokyo Kasei Kogyo Co., Ltd., Nissan Chemical Industries Ltd., and AZmax Co., Ltd., respectively. The diameter of colloidal silica particles was in the range of 10−20 nm. Also, 36% hydrochloric acid was purchased from Nacalai Tesque, Inc.

Preparation of Sol−Gel Films. TEOS, colloidal silica, and FOETES were used as starting materials for the preparation of sol−gel films. Variable amounts of colloidal silica and FOETES were added to the mixture of 4.61 mmol (0.96 g) of TEOS and 0.1 N HCl solution (0.19 mL), and they were stirred for 1/2 h using a magnetic stirrer at room temperature. Then, the solution was spin-coated onto substrates at room temperature using a Kyowariken K-369SD1 spin coater. When a slower rotation was applied for the spin-coating process, the uniformity in the sol−gel film was not good enough. Hence, a rotational speed of 2000 rpm and a holding time of 1 min were chosen. Then, the films were thermally treated at 423 K for 1 h. After removal of a part of the sol−gel membrane using a sharp blade, the step height was measured by atomic force microscopy (AFM), and was defined as the film thickness. The value so obtained was approximately 500 nm. The formation of the sol−gel film, namely, formation of the siloxane network, was confirmed on the basis of the time evolution of Si−O−Si absorption bands at around 1050, 1150, and 800 cm^{-1}, using Fourier transform infrared (FT-IR) spectroscopy.[30,31] The FT-IR spectra were recorded using a Perkin-Elmer Spectrum One spectrometer.

Surface Aggregation Structure and Wetting Properties. Surface aggregation states in the sol−gel films were studied by AFM, transmission electron microscopy (TEM), and angle-dependent X-ray photoelectron spectroscopy (ADXPS). AFM observation of the sol−gel films was carried out using an Explorer scanning probe microscope operated with a TM microscope TMX-2100 controller. The cantilever used was fabricated from Si_3N_4 and possessed a bending spring constant of 0.032 $N \cdot m^{-1}$. The normal force on the cantilever was as small as possible. To study the structure in the vicinity of the surface, TEM observation was also made for cross sections of the sol−gel films using a Hitachi H-7500 operated at an accelerating voltage of 100 kV. Thin sections with a thickness of 50−100 nm were microtomed with a diamond knife at room temperature. ADXPS measurement was carried out at a temperature lower than 223 K using a Physical Electronics 5800 spectrometer. Monochromatic Al Kα was used as an X-ray source. A C_{1s} peak corresponding to neutral carbons was assigned to a binding energy of 285.0 eV to correct for the charging energy shift. The analytical depth of XPS (d) from the outermost surface is defined by $3\lambda \sin \alpha$, where λ and α are the inelastic mean-free path of photoelectrons in a solid and the emission angle of photoelectrons, respectively. The inelastic mean-free path of photoelectrons was calculated by Ashley's equation.[32] The emission angle of photoelectrons was varied from 15° to 90° in this experiment.

Contact angles for the sol−gel films were measured at room temperature by the sessile drop method using a Krüss DSA 10 apparatus. Advancing and receding contact angles (θ_A and θ_R) were measured after the liquid droplet volume was increased to 4 μL or decreased to 2 μL, respectively. Water and dodecane were used as probe liquids. In addition, growth of water droplets at the surface and its roughness dependence were examined using an environmental scanning electron microscopy (ESEM) microscope, Nikon XL30, operated at an accelerating voltage of 20 kV. A specimen was placed in the vacuum chamber of the ESEM microscope and cooled to 273 K under a pressure of about 50 Pa. By increasing the relative humidity in the chamber to about 620 Pa, condensation of water vapor to the specimen surface was induced. For in situ observation of this process, the sample was tilted 40°.

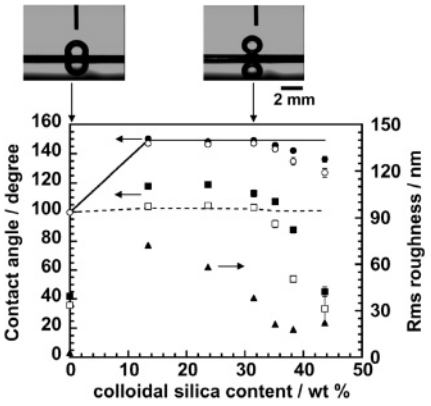

Figure 1. Colloidal silica content dependence of contact angles and surface roughness. The upper micrographs show water droplets on the surface of sol−gel films containing colloidal silica of 0 and 30 wt %: ●, θ_A for water; ○, θ_R for water; ■, θ_A for dodecane; □, θ_R for dodecane; ▲, rms roughness. Solid and dotted lines denote contact angles predicted by Cassie's and Wenzel's equations, respectively. See the text for details.

Results and Discussion

Colloidal silica particles and fluoroalkylsilane were used for controlling surface roughness and chemistry, respectively. A sol−gel film prepared by hydrolysis and condensation of alkoxysilane compounds is chosen to be the matrix of the film. In this paper, it is demonstrated how the combination between colloidal silica particles and fluoroalkylsilane makes it possible to construct sol−gel films with super-liquid-repellency.

Roughness Effect on Wetting Properties. Figure 1 shows the colloidal silica content dependences of the contact angle and surface roughness for the sol−gel films containing an FOETES fraction of 15 wt %. The surface roughness is expressed in terms of the root-mean-square roughness in Figure 1. Figure 2 illustrates the surface morphology for the films obtained by AFM.

As shown in Figure 1, contact angles to water and dodecane were 100° and 40°, respectively, for the surface without colloidal silica. Once the colloidal silica was added to the system, the surface morphology changed (Figure 2) and the measured contact angles for both probe liquids increased (Figure 1). At a silica content of 30 wt %, the silica particles seemed to be uniformly dispersed in the films. This is of importance to keep the transparency of the films, and is a key for practical use. At a colloidal

(30) Lee, M. S.; Jo, N. J. *J. Sol-Gel Sci. Technol.* **2002**, *24*, 175.
(31) Shirtcliffe, N. J.; McHale, G.; Newton, M. I.; Perry, C. C. *Langmuir* **2003**, *19*, 5626.
(32) Ashley, J. C. *IEEE Trans. Nucl. Sci.* **1980**, *NS-27*, 1454.

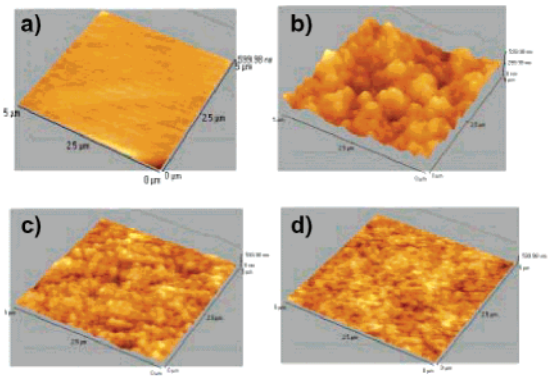

Figure 2. AFM images of sol−gel films containing colloidal silica of (a) 0 wt %, (b) 10 wt %, (c) 30 wt %, and (d) 40 wt %. The magnification is the same for all panels. An area of 5 × 5 μm^2 is shown, and the maximum height for the images was 600 nm.

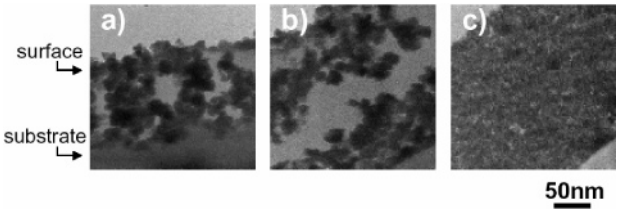

Figure 3. TEM images of sol−gel films containing colloidal silica particles of (a) 10 wt %, (b) 30 wt %, and (c) 40 wt %.

silica content of 10−30 wt %, both θ_A and θ_R to water were approximately 150°, and contact angle hysteresis defined as $\theta_A - \theta_R$ was practically not observed. Two CCD images in the upper part of Figure 1 show the shapes of water droplets on the coating with silica contents of 0 and 30 wt %, and visually present the above-mentioned discussion. Hence, it can be claimed that a superhydrophobic surface with excellent stability to water was successfully constructed in this silica content range.

In addition, the coating prepared with this silica content exhibited high contact angles for dodecane, approximately 120° (a few degrees of hysteresis was observed). The dodecane contact angle of 120° is one of the highest values reported so far. Interestingly, when the colloidal silica content went beyond 30 wt %, the surface of the sol−gel films became smoother, and the contact angles for water and dodecane decreased. Thus, it seems most likely that the super-liquid-repellent surfaces can be easily constructed by a one-pot process as long as the surface roughness is precisely optimized.

Figure 3 shows TEM images for sol−gel films prepared at colloidal silica contents of 10, 30, and 40 wt %. Darker regions correspond to colloidal silica particles. In panels a and b, aggregates with a size of around 50 nm are observed, aggregates composed of 2−5 silica particles. Hence, it is easy to understand why the surface roughness in the sol−gel films, especially at a silica content of 10−30 wt %, was much larger than the silica particle size. On the other hand, such aggregates were not observed for sol−gel films containing colloidal silica of 40 wt %.

We now turn to the relation of contact angle to surface roughness. According to the well-known Wenzel equation describing the contact angle θ on a rough surface, the θ value increases with increasing surface area as follows:

$$\cos \theta = r \cos \theta_{flat} \quad (1)$$

Here, r is the roughness parameter defined as the ratio of real surface area to projected surface area and θ_{flat} is

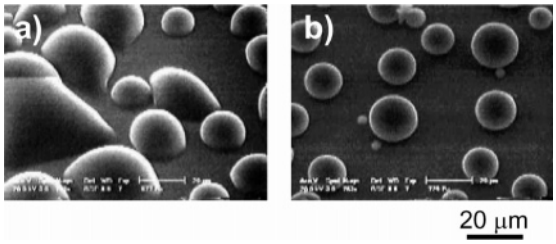

Figure 4. ESEM images showing surface condensation of water vapor for sol−gel films (a) without and (b) with colloidal silica.

the contact angle measured on a flat surface. In our system, the contact angle for the sol−gel film without colloidal silica particles was $\theta_{flat} = 100°$. At a colloidal silica content from 10 to 30 wt %, r was evaluated to be within the range from 1.24 to 1.28 as determined with AFM. Then, θ was calculated to be 102.4−102.8° (shown as a dotted line in Figure 1). These values are much lower than what we experimentally obtained. When the surface roughness exceeds a certain level, the wetting behavior actually transits to a regime in which the liquid does not penetrate into the grooves.[9−12] This has been recognized as the notion of heterogeneous wetting proposed by Cassie. In this case, the space between the solid surface and probe liquid is, of course, occupied by air. Since the liquid contact angle with air should be equal to 180°, θ of the heterogeneous surface composed of the solid and the air phase is described as follows:

$$\cos \theta = (f \cos \theta_{flat}) + f - 1 \quad (2)$$

where f is the area fraction of the solid in contact with the liquid. When an f value of about 0.15 was taken for eq 2, θ of 150° corresponding to the experimental value was obtained. This analysis implies that water did not penetrate the surface grooves on the sol−gel films prepared at a silica content from 10 to 30 wt %, although the effect of the groove geometry on the contact angles[9−12] should also be taken into account in more detailed analysis.

The condensation of water droplets on the film surface was also studied. A sample was placed in the vacuum chamber of the ESEM microscope and cooled to 273 K. After a given time, the relative humidity in the chamber was increased. Figure 4 shows snapshots upon surface condensation of water vapor on the sol−gel films without and with the colloidal silica. The shape and size of the water droplets were monodispersed for the sol−gel film containing colloidal silica of 30 wt %, whereas in the case of the film without colloidal silica, they were quite distributed. Thus, it can be envisaged that the condensation of water vapor is also affected by the surface roughness.

Chemical Effect on Wetting Properties. After discussion about the roughness effect on wettability, we turn to optimization of the fluorine amount fed into the coating. On the basis of the results discussed in previous sections, the sol−gel films were prepared at a silica content of 30 wt % and varying amounts of FOETES. Figure 5 shows how the bulk FOETES content affects the contact angle and surface fluorine concentration of the sol−gel films. To what extent fluorine atoms exist in the surface region is expressed in terms of the atomic ratio of fluorine and silicon (F/Si), which is accessible by X-ray photoelectron spectroscopy (XPS). Although the F/Si value increased with increasing FOETES fraction, the contact angles remained constant at an FOETES fraction higher than 15 wt %. This means that the coverage of fluoroalkyl groups at the outermost surface was saturated at this fraction.

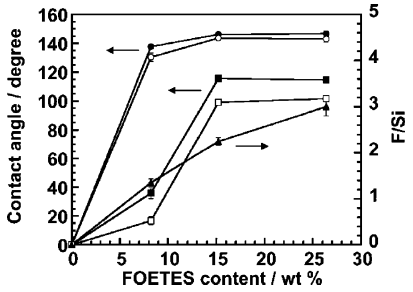

Figure 5. FOETES content dependence of contact angles and F/Si atomic ratio: ●, θ_A for water; ○, θ_R for water; ■, θ_A for dodecane; □, θ_R for dodecane; ▲, F/Si.

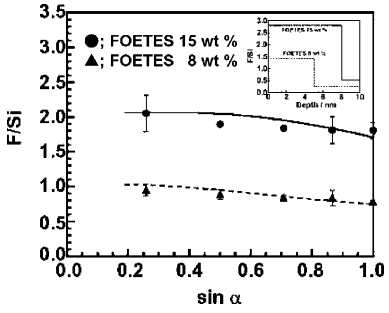

Figure 6. Relationship between sin α and F/Si for sol−gel films containing various FOETES contents. Symbols are experimental data sets, and solid and dotted lines are the best-fit ones calculated on the basis of model depth profiles shown in the inset.

To study the depth profile of FOETES molecules for the coating, ADXPS measurements were carried out.[33] Figure 6 shows the relation between F/Si and sin α, where α is the emission angle of photoelectrons. Hence, a smaller sin α means a shallower analytical depth. In both cases, the F/Si value slightly increased with decreasing sin α, implying that the fluoroalkyl groups are enriched in the surface region. The surface fluorine content for the film containing FOETES of 8 wt % was always lower than that of the one containing FOETES of 15 wt % at a given sin α. In the XPS measurement, photoelectrons are not uniformly emitted from a given analytical depth region. Instead, the detected amount of photoelectrons exponentially decays with increasing depth, meaning that the relation of the F/Si value and sin α cannot be simply regarded as the depth profile of fluorine. Hence, extraction of a plausible depth profile of F/Si near the surface was attempted on the basis of Paynter's analysis.[34] In this method, the surface region is first divided into compositionally uniform parallel layers. Since the intensity of photoelectrons from the multilayer can be given by eq 3,

$$I(\alpha,x) = Fk\left(\int_0^{x_1}\exp\left(-\frac{x}{\lambda \sin \alpha}\right)n_1\,dx + \int_{x_1}^{x_2}\exp\left(-\frac{x}{\lambda \sin \alpha}\right)n_2\,dx + \int_{x_2}^{x_3}\exp\left(-\frac{x}{\lambda \sin \alpha}\right)n_3\,dx + ...\right) \quad (3)$$

where n_i is the number density of atoms in a homogeneous layer from x_i to x_{i+1}, the plausible depth profile of F/Si is obtained. When the depth profiles shown in the inset of Figure 6 were taken, the experimental data were well fit, as drawn by the solid and dotted lines in Figure 6. Invoking

(33) In general, ADXPS measurement is made under the assumption that the surface is perfectly smooth. However, the surface in the sol−gel films was rough in reality. This may interfere with the quantitative analysis, although the essential discussion would not be altered.

(34) Paynter, R. W. *Surf. Interface Anal.* **1981**, *3*, 186.

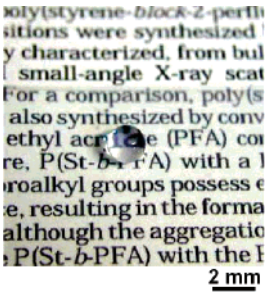

Figure 7. CCD image of a water droplet on a PET film coated with a sol−gel film.

that the inset reflects the real F/Si−depth relations, it can be claimed that the fluoroalkyl layer is formed at the surface in both films, and that the surface layer with a lower energy was thicker in the film with an FOETES fraction of 15 wt % than in the one with an FOETES fraction of 8 wt %.

Application of Sol−Gel Films. Sol−gel films can be basically coated onto any solid substrate. In this study, a transparent polymer film of poly(ethylene terephthalate) (PET) was used as the substrate. Figure 7 shows a water droplet on the PET film with the sol−gel coating layer, which was prepared at a colloidal silica content of 30 wt % and an FOETES content of 15 wt %. The surface roughness of the coating layer was almost the same as that for the sol−gel film on the silicon wafer, and was approximately 30 nm. Concurrently, contact angles for water and dodecane were almost identical to the values for the sol−gel film on the silicon wafer. That is, the PET film with a sol−gel surface layer exhibited super-liquid-repellent properties. In addition, the transmittance of visible light through the PET film coated with a sol−gel layer remained at more than 80%. This enables us to read text printed beneath the film, as shown in Figure 7.

The durability of the sol−gel layer, which should be one of the crucial factors for practical use, was examined by rubbing the surface with a piece of cloth under a load of 240 Pa. After such a test, the surface roughness was not altered within experimental accuracy, implying that the durability of the layer coated was acceptable for practical use as well.

Conclusions

Super-liquid-repellent surfaces were successfully fabricated in this study using one-step sol−gel coating technology. We prepared sol−gel films containing colloidal silica nanoparticles and fluoroalkylsilane coupling agent, which were responsible for controlling surface energy and roughness. These films demonstrated 150° and 120° contact angles for water and dodecane, respectively. We expect that any solid substrate with a large area could be uniformly coated with sol−gel films, and therefore, this technology should have a great practical potential. Important properties of super-liquid-repellent coating are its transparency and durability.

Acknowledgment. We are most grateful for helpful discussion with Professor Toshihiko Nagamura, Kyushu University. This study was carried out as the "Nanostructure Polymer Project" supported by NEDO (New Energy and Industrial Technology Development Organization) launched in 2001.

LA050901R